SPANDIDOS PUBLICATIONS

MOLECULAR MEDICINE REPORTS 28: 187, 2023

Gleditsiae fructus regulates osteoclastogenesis by inhibiting the c-Fos/NFATc1 pathway and alleviating bone loss in an ovariectomy model

CHANG-YOUNG CHO*, SE HWANG KANG*, BYUNG-CHAN KIM, TAE-KYU KIM, JAE-HYUN KIM, MINSUN KIM, YOUNGJOO SOHN and HYUK-SANG JUNG

Department of Anatomy, College of Korean Medicine, Kyung Hee University, Seoul 02-447, Republic of Korea

Received May 24, 2023; Accepted July 21, 2023

DOI: 10.3892/mmr.2023.13074

Abstract. Medical and economic developments have allowed the human lifespan to extend and, as a result, the elderly population has increased worldwide. Osteoporosis is a common geriatric disease that has no symptoms and even a small impact can cause fractures in patients, leading to a serious deterioration in the quality of life. Osteoporosis treatment typically involves bisphosphonates and selective estrogen receptor modulators. However, these treatments are known to cause severe side effects, such as mandibular osteonecrosis and breast cancer, if used for an extended period of time. Therefore, it is essential to develop therapeutic agents from natural products that have fewer side effects. *Gleditsiae fructus* (GF) is a dried or immature fruit of *Gleditsia sinensis* Lam. and is composed of various triterpenoid saponins. The anti-inflammatory effect of GF has been confirmed in various diseases, and since the anti-inflammatory effect plays a major role in inhibiting osteoclast differentiation, GF was expected to be effective in osteoclast differentiation and menopausal osteoporosis; however, to the best of our knowledge, it has not yet been studied. Therefore, the present study was designed to examine the effect of GF on osteoclastogenesis and to investigate the mechanism underlying inhibition of osteoclast differentiation. The effects of GF on osteoclastogenesis were determined *in vitro* by tartrate-resistant acid phosphatase (TRAP) staining, pit formation assays, filamentous actin (F-actin) ring formation assays, western blotting and reverse transcription-quantitative PCR analyses. Furthermore, the administration of GF to an animal model exhibiting menopausal osteoporosis allowed for the analysis of alterations in the bone microstructure of the femur using micro-CT. Additionally, assessments of femoral tissue and serum were conducted. The present study revealed that the administration of GF resulted in a reduction in osteoclast levels, F-actin rings, TRAP activity and pit area. Furthermore, GF showed a dose-dependent suppression of nuclear factor of activated T-cells cytoplasmic, c-Fos and other osteoclastogenesis-related markers.

Correspondence to: Professor Hyuk-Sang Jung, Department of Anatomy, College of Korean Medicine, Kyung Hee University, 26-6 Kyungheedae Road, Dongdaemun, Seoul 02-447, Republic of Korea
E-mail: jhs@khu.ac.kr

*Contributed equally

Key words: *Gleditsiae fructus*, osteoclast, nuclear factor of activated T-cells cytoplasmic 1, c-Fos, ovariectomy

Introduction

As the lifespan of human beings extends due to medical and economic developments, the worldwide elderly population is increasing (1,2). Due to this, the frequency of patients with age-related osteoporosis and mortality from osteoporotic fractures is also rapidly increasing (3). Bone is a dynamic tissue that undergoes destruction and recreation throughout a human's lifespan and requires a balance of osteoclasts and osteoblasts (4). Osteoporosis occurs when the excessive activity of osteoclasts, responsible for bone destruction, outbalances the activity of osteoblasts, responsible for bone formation (5). Osteoporosis is asymptomatic, but even a relatively small impact can cause fractures in patients, leading to a serious deterioration in the quality of life (6). Osteoporosis treatment typically involves bisphosphonates and selective estrogen receptor modulators (SERMs) (7). However, these treatments have adverse side effects, with long-term use of bisphosphonate causing mandibular osteonecrosis and cardiovascular disease, and SERM treatment known to cause serious side effects, such as breast cancer (8,9). Therefore, the development of alternative therapeutic agents from natural products with fewer side effects is essential.

Osteoclasts are formed from hematopoietic precursors of the monocyte/macrophage lineage (10) and are responsible for bone resorption. The cytokine, receptor activator of nuclear factor-κB ligand (RANKL), is crucial for osteoclastogenesis (11). The binding of RANKL to the cell surface receptor, RANK, triggers a signaling cascade that involves TNF receptor associated factor 6 (TRAF6), ultimately leading to the activation of essential transcription factors for osteoclastogenesis, including nuclear factor of activated T cells 1 (NFATc1) and c-Fos (12-14). The activation of

NFATc1 induces osteoclastogenesis-related markers, such as tartrate-resistant acid phosphatase (TRAP), carbonic anhydrase type II (CA2) and ATPase H+ transporting V0 subunit d2 (ATP6v0d2) (15-17). Therefore, inhibition of the RANK-RANKL signaling pathway is a major therapeutic target for osteoporosis.

Gleditsiae fructus (GF) is the dried or immature fruit of *Gleditsia sinensis* Lam. and has been traditionally used for the management of inflammation and injury. GF is abundant in triterpenoid saponins, a class of glycosides widely found in the plant realm (18). Saponins possess noteworthy properties including anti-inflammatory, analgesic, antioxidant and hydrogen peroxide scavenging effects (19). Moreover, saponins play a key role in promoting cell regeneration, particularly in keratinocytes. Amongst the saponins, echinocystic acid and oleanolic acid are known to be active components of GF (20), with echinocystic acid displaying anti-inflammatory and antioxidant effects (21,22), and oleanolic acid demonstrating anti-inflammatory and antiallergic effects through inhibition of the transcriptional regulation of MAPKs and NF-κB (23,24). Oleanolic acid has also been shown to inhibit osteoclastogenesis and bone loss (25). The expression of inflammatory cytokines is an osteoclast activation factor and has been reported to be one of the causes of metabolic bone disease (26). Therefore, it was inferred that GF could be effective for the treatment of osteoporosis. However, to the best of our knowledge, the effect of GF on osteoclast differentiation and postmenopausal osteoporosis has not yet been elucidated. Therefore, the present study aimed to investigate the effect of GF on osteoclastogenesis, identify the NFATc1/c-fos-mediated osteoclastogenesis pathway and confirm the promoting effect of GF on osteoblasts. Additionally, the inhibitory effect of GF on bone density reduction was evaluated and the mechanism underlying the anti-osteoporosis effect of GF in the ovariectomy (OVX) model was elucidated.

Materials and methods

Reagents. Dulbecco's Modified Eagle's Medium (DMEM) and Dulbecco's PBS (DPBS) were acquired from Welgene, Inc. α-Minimum essential medium (α-MEM) and penicillin/streptomycin (P/S) were acquired from Gibco (Thermo Fisher Scientific, Inc.). Fetal bovine serum (FBS) was purchased from Atlas Biologicals, Inc. RANKL was purchased from PeproTech EC Ltd. Cell Counting Kit-8 (CCK-8) was acquired from Dojindo Laboratories, Inc. TRAP staining kits, bicinchoninic acid (BCA) solution, 17b-estradiol (E_2), alendronate (ALN) and 4',6-diamidino-2-phenylindole (DAPI) were obtained from Sigma-Aldrich (Merck KGaA). Acti-stain™ 488 Fluorescent Phalloidin was obtained from Cytoskeleton, Inc. Osteo assay strip well plates were acquired from Corning, Inc. PCR primers were purchased from GenoTech Corp. Primary and secondary antibodies were as follows: β-actin (sc-8432; Santa Cruz Biotechnology, Inc.), NFATc1 (cat. no. 556602; BD Biosciences), c-Fos (cat. no. sc-447; Santa Cruz Biotechnology, Inc.), matrix metalloprotease 9 (MMP-9; cat. no. ab38898; Abcam), cathepsin K (CTK; cat. no. ab19027; Abcam), peroxidase AffiniPure Goat Anti-Mouse IgG (cat. no. 115-035-062; Jackson ImmunoResearch Laboratories, Inc.) and peroxidase AffiniPure Goat Anti-Rabbit IgG (cat. no. 115-035-144; Jackson ImmunoResearch Laboratories, Inc.).

Preparation of GF ethanol extract. GF (100 g) purchased from Omni Herb, Co., Ltd. was immersed in a liter of 30% ethanol at 4˚C for 3 weeks and sonicated (40 kHz) once every 2 days at room temperature for 1 h. The resulting mixture was filtered using no. 3 filter paper (Whatman plc; Cytiva), and the filtrate was concentrated using a rotary evaporator. Finally, the concentrated extract was freeze-dried into a powder with a yield of 15.9% (15.9 g powder). The resulting powder was stored at -20˚C until further use.

Cell culture and cytotoxicity measurement. RAW 264.7 cells were obtained from The Korean Cell Line Bank (Korean Cell Line Research Foundation) and MC3T3-E1 cells from the American Type Culture Collection (cat. no. ATCC-CRL-2593). RAW 264.7 cells were cultured in DMEM supplemented with 10% FBS and 1% P/S and subcultured every 2 days in a humidified incubator (Thermo Fisher Scientific, Inc.) at 37˚C and 5% CO_2. MC3T3-E1 cells were cultured in α-MEM (without ascorbic acid), supplemented with 10% FBS and 1% P/S and subcultured every 3 days in a humidified incubator at 37˚C and 5% CO_2. To evaluate the cytotoxicity of GF, 5,000 RAW 264.7 and 5,000 MC3T3-E1 cells were seeded in 96-well plates and allowed to stabilize for 24 h. Various concentrations of GF (0, 5, 10, 20 and 40 μg/ml) were then added to the cells and the cells were incubated for a further 24 h. After treatment, 20 μl CCK-8 solution was added to each well and the plates were incubated for an additional 2 h. Cell viability was determined by measuring the absorbance at 450 nm using an enzyme-linked immunosorbent assay (ELISA) plate reader. The results were expressed as a percentage of the untreated cell control and a survival rate ≤90% compared with the control was considered indicative of toxicity.

TRAP staining and TRAP activity. To evaluate the inhibitory effect of GF on osteoclast formation, RAW 264.7 cells were seeded at a density of 5,000 cells/well in 96-well plates and incubated for 24 h. The cells were then treated with 100 ng/ml RANKL, which is an osteoclastogenesis-inducing cytokine, and various concentrations of GF (0, 5, 10, 20 and 40 μg/ml) for 5 days with medium changes on days 2 and 4. After fixation with 4% formalin for 1 h at the room temperature, TRAP staining was performed for 1 h at the room temperature and TRAP (+) cells with ≥3 nuclei were counted using ImageJ software v1.46 (National Institutes of Health) under an inverted microscope (magnification, x100). In addition, the activity of TRAP in the culture medium was measured by mixing an equal volume of TRAP solution (4.93 mg p-nitrophenyl phosphate in 750 ml 0.5 M acetate solution and 150 ml tartrate acid solution) with the medium on day 5 and then incubated for 1 h. Finally, the reaction was stopped with NaOH and the absorbance at 405 nm was measured using an ELISA plate reader.

Pit formation and filamentous actin (F-actin) ring formation assays. To confirm the effect of GF on the inhibition of bone resorption ability, 5,000 RAW 264.7 cells were seeded into osteo assay strip well plates and stabilized for 24 h at 37˚C. The cells were treated with RANKL (100 ng/ml) and various concentrations of GF (0, 5, 10, 20 and 40 μg/ml) for 5 days at 37˚C. The culture medium was exchanged on days 2 and 4

with the same medium. Then, the cells were removed using 4% sodium hypochlorite. The area of the pit in the plate was measured using ImageJ software v1.46 and the area in the plate absorbed by osteoclasts was expressed as a percentage of the total area.

To determine the effect of GF on actin ring formation, 5,000 RAW 264.7 cells were seeded into 96-well plates and stabilized for 24 h. The cells were treated with RANKL (100 ng/ml) and various concentrations of GF (0, 5, 10, 20 and 40 μg/ml) for 5 days at 37˚C. The culture medium was exchanged on days 2 and 4 with the same medium. After the formation of osteoclasts, the cells were fixed using 4% paraformaldehyde for 10 min at room temperature and then permeabilized with 0.1% Triton™ X-100 in PBS for 5 min at room temperature. The cells were then incubated with Acti-stain™ 488 fluorescent phalloidin and DAPI in the dark for 30 min at room temperature. The actin rings were visualized using a fluorescence microscope (magnification, x200) and the number of actin rings was quantified using ImageJ software v1.46.

Western blot analysis. RAW 264.7 cells were seeded at a density of $5x10^5$ cells per 60 mm dish and allowed to stabilize for 24 h. The cells were then treated with RANKL (100 ng/ml) and different concentrations of GF (0, 5, 10, 20 and 40 μg/ml) for 24 h to confirm the effect of GF on transcription factors related to osteoclastogenesis. After treatment, the cells underwent a DPBS wash, and the total protein was extracted from the cells using RIPA buffer (50 mM Tris-Cl, 150 mM NaCl, 1% NP-40, 0.5% sodium deoxycholate and 0.1% SDS) containing protease and phosphatase inhibitors (1:100; Sigma-Aldrich; Merck KGaA), to obtain a comprehensive protein profile. The protein concentration was quantified using the BCA assay and 30 μg protein/lane was separated by SDS-PAGE on 10% gels, before being transferred onto nitrocellulose membranes. The membranes were blocked with TBS-0.5% Tween 20 containing 5% skim milk to minimize non-specific protein binding for 1 h at room temperature, and then incubated with primary antibodies overnight at 4˚C (NFATc1, 1:1,000; c-Fos, 1:200; β-actin, 1:1,000) and then with secondary antibodies (1:10,000) for 1 h at room temperature. Finally, the bands were visualized using ECL solution (Cytiva) and their density was measured using ImageJ v1.46. The protein expression levels were then normalized to those of the loading control (β-actin).

Reverse transcription-PCR (RT-PCR). To confirm the effect of GF on osteoclastogenesis-related transcription factors, $2x10^5$ RAW 264.7 cells were seeded in 6-well plates and stabilized for 24 h. Cells were treated with RANKL (100 ng/ml) and various concentrations of GF (0, 5, 10, 20 and 40 μg/ml) for 4 days. Next, the cells were washed with DPBS three times and total RNA was extracted using TRIzol® reagent (Takara Bio, Inc.). The NanoDrop 2.0 spectrophotometer (NanoDrop Technologies; Thermo Fisher Scientific, Inc.) was utilized to quantify 2 μg of extracted RNA. Subsequently, cDNA was synthesized in accordance with the manufacturer's protocol provided by the RT kit (Invitrogen; Thermo Fisher Scientific, Inc.), followed by its amplification with Taq polymerase (Kapa Biosystems; Roche Diagnostics). The PCR conditions were as follows: Denaturation for 30 sec at 94˚C, annealing for 30 sec at 53-58˚C and extension for 30 sec at 72˚C. Primer sequences and number of cycles for each gene are listed in Table I. mRNA expression levels were normalized to that of the loading control (β-actin). The RT-PCR results were confirmed using a 2% agarose gel stained with SYBR Green (1:10,000; Invitrogen; Thermo Fisher Scientific, Inc.). The density of the bands was measured using ImageJ v1.46.

Animals and OVX model. A total of 48 Sprague Dawley 11-week-old female rats were obtained from Nara Biotech (mean weight 240±10 g) and the animals were stabilized in a new environment for 1 week. All animals were raised in a specific pathogen-free environment, including a temperature of 20-24˚C and humidity of 50-60%, under a 12 h light/dark cycle. All animals had *ad libitum* access to food and water and the animal experiments were approved by The Kyung Hee University Institutional Animal Care and Use Committee (Seoul, Republic of Korea; approval no. KHSASP-21-185). The postmenopausal osteoporosis model was induced by OVX. For this, all animals were subjected to deep anesthesia in 100% oxygen with 5% isoflurane before undergoing bilateral OVX. The concentration of isoflurane was maintained at 2-3% during surgery. Animals in the sham group underwent the same surgical procedure with identical stress levels but without bilateral OVX. After surgery, 4 mg/kg gentamycin was injected for 3 days to prevent infection at the wound site. The animal groups (n=8/group) comprised the following: i) Sham group, animals subjected to sham operation and orally administered distilled water; ii) OVX group, animals subjected to OVX and orally administered distilled water; iii) E_2 group, animals subjected to OVX and orally administered 100 μg/kg E_2; iv) ALN group, animals subjected to OVX and orally administered 3 mg/kg ALN; v) low GF (GF-L) group, animals subjected to OVX and orally administered 21.147 mg/kg GF; and vi) high GF (GF-H) group, animals subjected to OVX and orally administered 135.34 mg/kg GF. The concentration of administered GF was determined as per the following procedure. In Korean medicine, the average amount of GF consumed by a 60 kg adult per day is 8 g (27). The yield of GF is 15.9%. The calculated dose to be administered in the GF-L group was 21.147 mg/kg. It is known that the metabolism of rats is 6.4x faster than that of humans (28). Therefore, the GF-H group was administered 135.34 mg/kg. In the present study, two drugs were used as positive controls to compare the anti-osteoporotic effects of GF. The first is E_2, which is commonly used to treat osteoporosis in postmenopausal women. The second is ALN, which is a bisphosphonate agent used to treat osteoporosis (29), preventing bone destruction and increasing bone thickness. The change in body weight of animals was measured once a week and drug administration was performed for a total of 8 weeks. The health status of the rats was checked twice daily. The humane endpoints of this study were set as follows: i) Inability to eat, ii) rapid weight loss of 20% or more in 1 week, iii) immobility. During the experiment, no abnormal changes in health were observed in all of the rats. After 8 weeks, all animals were sacrificed by lethal cardiac puncture up to 10 ml (30), under deep anesthesia in 100% oxygen and 5% isoflurane. Subsequently, after confirming that the hearts of all animals had completely stopped, cervical dislocation was performed.

Table I. Primer sequences for reverse transcription PCR.

Gene name	Primer sequence (5'-3')	Tm, °C	No. of cycles	Accession no.
NFATc1 (*Nfatc1*)	Forward: TGCTCCTCCTCCTGCTGCTC Reverse: CGTCTTCCACCTCCACGTCG	58	32	NM_198429.2
c-Fos (*Fos*)	Forward: ATGGGCTCTCCTGTCAACAC Reverse: GGCTGCCAAAATAAACTCCA	58	33	NM_010234.3
TRAP (*Acp5*)	Forward: ACTTCCCCAGCCCTTACTACCG Reverse: TCAGCACATAGCCCACACCG	58	30	NM_007388.3
RANK (*Tnfrsf11a*)	Forward: AAACCTTGGACCAACTGCAC Reverse: ACCATCTTCTCCTCCCGAGT	53	32	NM_009399.3
MMP-9 (*Mmp9*)	Forward: CGACTTTTGTGGTCTTCCCC Reverse: TGAAGGTTTGGAATCGACCC	58	30	NM_013599.4
CA2 (*Ca2*)	Forward: CTCTCAGGACAATGCAGTGCTGA Reverse: ATCCAGGTCACACATTCCAGCA	58	32	NM_001357334.1
OSCAR (*Oscar*)	Forward: CTGCTGGTAACGGATCAGCTCCCCAGA Reverse: CCAAGGAGCCAGAACCTTCGAAACT	53	35	NM_001290377.1
ATP6v0d2 (*Atp6v0d2*)	Forward: ATGGGGCCTTGCAAAAGAAATCTG Reverse: CGACAGCGTCAAACAAAGGCTTGTA	58	30	NM_175406.3
DC-STAMP (*Dcstamp*)	Forward: TGGAAGTTCACTTGAAACTACGTG Reverse: CTCGGTTTCCCGTCAGCCTCTCTC	63	30	NM_001289506.1
β-actin (*Actb*)	Forward: TTCTACAATGAGCTGCGTGT Reverse: CTCATAGCTCTTCTCCAGGG	58	30	NM_008084.3

NFATc1, nuclear factor of activated T cells 1; TRAP, tartrate-resistant acid phosphatase; RANK, receptor activator of nuclear factor-κB; MMP-9, matrix metalloproteinase-9; CA2, carbonic anhydrase type II; OSCAR, osteoclast-associated receptor; ATP6v0d2, ATPase H+ transporting V0 subunit d2; DC-STAMP, Dendritic cell-specific transmembrane protein.

Biochemical assays using rat serum. Following whole blood extraction and reaction in an serum separator tube for 30 min at room temperature, the serum was separated through centrifugation (14,310 x g, 4°C, 10 min) and TRAP activity of the serum was assessed as aforementioned. The expression of alkaline phosphatase (ALP), aspartate aminotransferase (AST) and alanine transferase (ALT) was analyzed by DkKorea, an animal serum analysis company.

Microcomputed tomography (Micro-CT) analysis. The femurs of all animals were harvested 8 weeks after surgery and immersed in 10% neutral buffered formalin (NBF) at room temperature for 24 h to fix the bone tissue. Bone mass and microstructure were then evaluated by micro-CT using SkyScan1176 (Skyscan; Bruker Corporation) under the following conditions: An aluminum filter of 0.5 mm, 8.9 μm pixel size and a rotation angle of 180° with rotation steps of 0.4°. The analyzed bone parameters included bone mineral density (BMD), bone volume/total volume (BV/TV), trabecular thickness (Tb.Th) and trabecular separation (Tb.Sp).

Histological analysis. The femurs of all animals were harvested 8 weeks after surgery and fixed in 10% NBF at room temperature for 24 h. Subsequently, the femurs were demineralized in ethylenediaminetetraacetic acetic acid (pH 7.4) for 3 weeks and embedded in paraffin. Tissue sections of 5 μm thickness were obtained using a Zeiss rotary microtome and the sections were air-dried for 1 day. Hematoxylin-eosin (H&E) staining was used to analyze histomorphological changes. In brief, paraffin-embedded tissue sections were subjected to deparaffinization using xylene and ethanol, followed by counterstaining with eosin for 10 sec and hematoxylin for 5 min. For immunohistochemistry (IHC) staining, initially, the paraffin-embedded tissue underwent deparaffinization using a combination of xylene and ethanol. After that, antigen retrieval was performed using proteinase K (0.4 mg/ml) at 37°C for 30 min. Subsequently, 0.3% H_2O_2 (w/v) in Mt-OH was added at room temperature for 30 min to inhibit the activity of endogenous peroxidases, and 5% goat serum (Gibco; Thermo Fisher Scientific, Inc.) in PBS was used to prevent the binding of non-specific proteins for 1 h at room temperature. The tissues were incubated overnight at 4°C with primary antibodies NFATc1 (diluted 1:100) and CTK (diluted 1:100). The sections were then incubated with the secondary antibody (cat. no. BA-1000; Vector Laboratories, Inc.; Maravai LifeSciences) for 1 h at room temperature. The signal was detected using the ABC kit (Vector Laboratories, Inc.; Maravai LifeSciences) at room temperature for 30 min and visualized with 3,3-diaminobenzidine (DAB solution; cat. no. SK-4100; Vector Laboratories, Inc.; Maravai LifeSciences) at room temperature for 10 min. The stained tissues were analyzed using a light microscope (Olympus Corporation) and the trabecular area and positive cells were measured using ImageJ software v1.46.

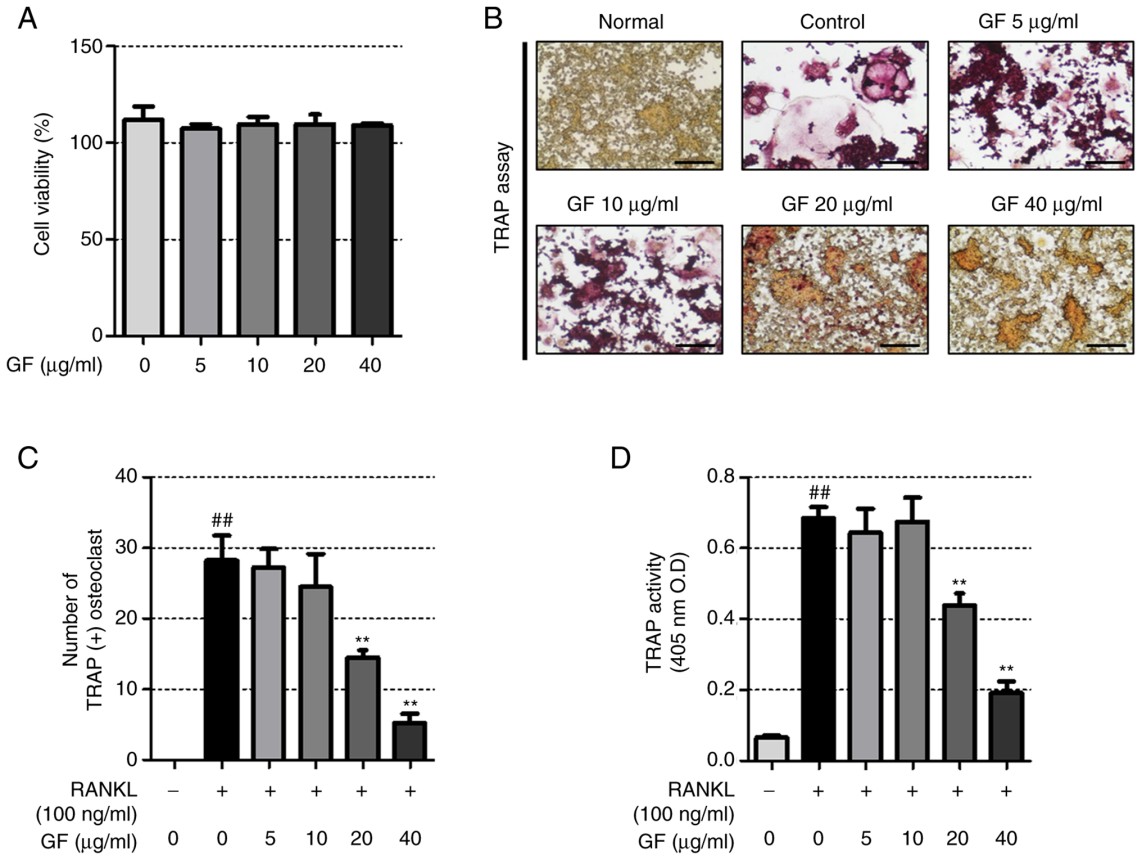

Figure 1. Effect of increasing doses of GF on osteoclastogenesis. (A) Cell viability was determined using the Cell Counting Kit-8 assay. (B) Cells were stained with a TRAP staining kit (magnification, x100; scale bar, 200 μm). Osteoclasts were stained bright red. (C) The number of TRAP (+) cells with >3 nuclei were counted using ImageJ software. (D) TRAP activity was measured at a wavelength of 405 nm in a Versamax plate reader after adding TRAP solution to the culture medium. All experiments were repeated at least 3 times and the results are expressed as the mean ± SEM. Statistical significance was verified by one-way ANOVA and Tukey's post hoc test. $^{##}$P<0.01 vs. normal, untreated cells; **P<0.01 vs. RANKL-induced cells. GF, *Gleditsiae fructus*; TRAP, tartrate-resistant acid phosphatase; RANKL, receptor activator of nuclear factor-κB ligand; O.D., optical density.

Alizarin red S staining. Alizarin red S staining was conducted to investigate the impact of GF on osteoblast formation and the formation of calcified nodules. A 6-well plate was seeded with $3x10^5$ MC3T3-E1 cells and incubated for 24 h. In order to differentiate MC3T3-E1 cells into osteoblasts, the cells were treated with ascorbic acid (A.A; 25 μg/ml), β-glycerol phosphate (B.G.P; 10 mM) and various concentrations of GF (0, 5, 10, 20 and 40 μg/ml) at 37˚C for 2 weeks. The culture medium was replaced every 3 days. Once calcified nodules were visible on the plate, the medium was removed and the cells were washed three times with cold PBS. The cells were then fixed with 80% ethanol at 4˚C for 1 h and stained with alizarin red S dye at room temperature for 30 min. Finally, images of the plate were captured using a digital camera (Canon, Inc.). The degree of dye staining was measured by extracting the dye using 10% (v/w) cetylpyridinium chloride in sodium phosphate and measuring the absorbance at 570 nm.

High-performance liquid chromatography analysis. Echinocystic acid and oleanolic acid are active ingredients of GF (20) and were purchased from Sigma-Aldrich (Merck KGaA). To analyze the GF extract, the absorbance was measured using a UV detector (2695 HPLC system with 2996 PDA detector; Waters Corp.), the flow rate was 1 ml and the operating time was 45 min using an Xbridge C18 (250x4.6 mm, 5 μm; Waters Corp.) column at the room temperature. The sample insertion volume was 10 μl. Solvent A of the mobile phase was acetonitrile and solvent B was water with 0.1% formic acid. The gradient program was as follows. 0 min, 5% B; 0-30 min, 5-50% B; 30-60 min, 50-95% B.

Statistical analysis. All data are presented as the mean ± standard error of mean. All experiments were repeated at least 3 times. Comparisons were conducted with one-way ANOVA and Tukey's post hoc test. P<0.05 was considered to indicate a statistically significant difference. Statistical analysis was performed using GraphPad PRISM v5.01 (Dotmatics).

Results

GF inhibits RANKL-induced osteoclastogenesis. To determine the effect of GF on RAW 264.7 cell cytotoxicity, a CCK-8 assay was performed that showed that GF did not induce RAW 264.7 cell cytotoxicity (Fig. 1A). The impact of GF on osteoclastogenesis in RAW 264.7 cells was also investigated by analyzing TRAP activity and performing TRAP staining. The results showed that RANKL-treated cells had a greater number of TRAP (+) cells and higher TRAP activity compared with untreated cells, while GF reduced

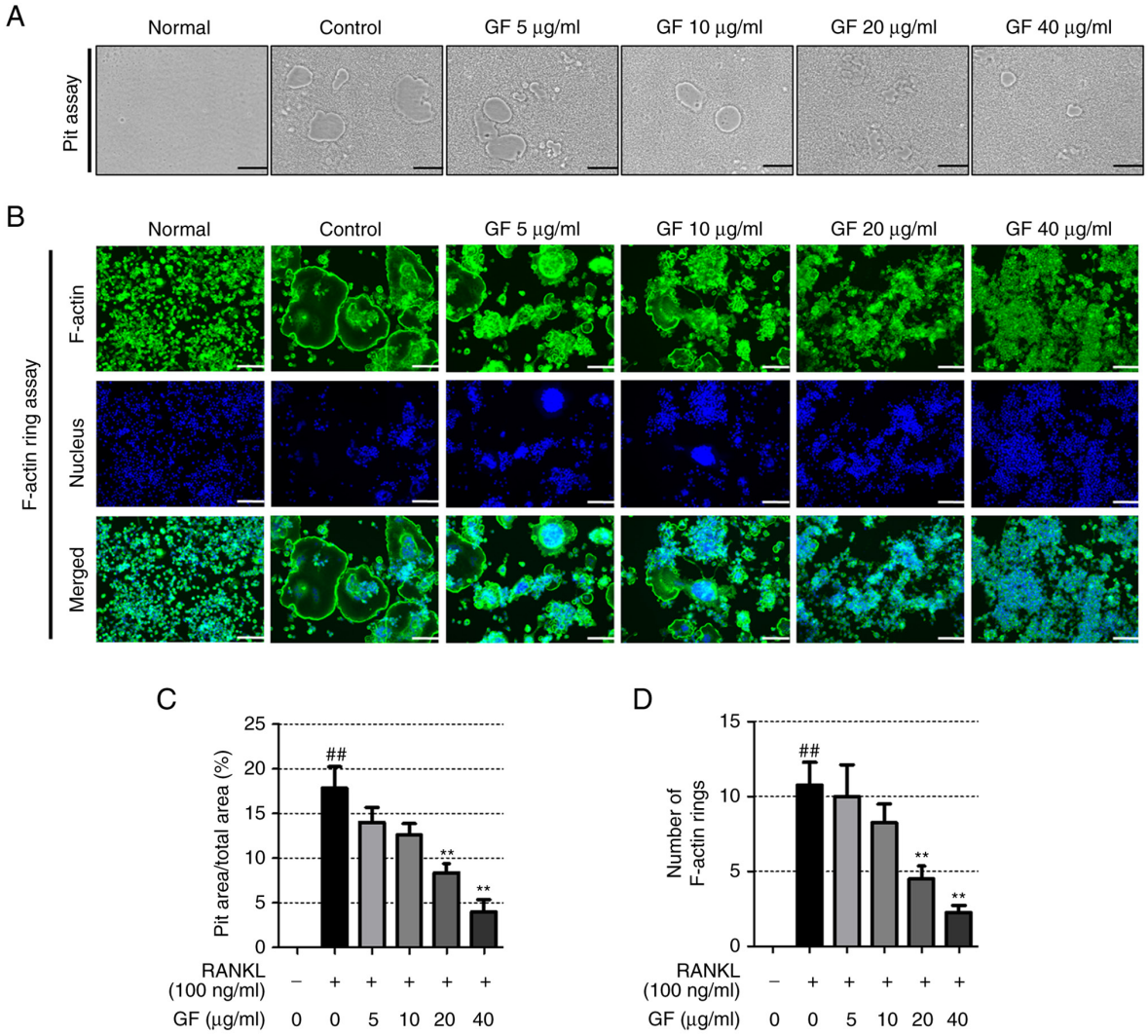

Figure 2. Effect of increasing doses of GF on pit formation and F-actin ring formation. (A) Images of the formed pit were captured using an optical inverted microscope (magnification, x100, scale bar, 200 μm). (B) Images of the F-actin ring were captured using an immunofluorescence microscope (magnification, x100, scale bar, 200 μm). (C) The area of the pit and (D) the number of F-actin rings were counted using ImageJ software. All experiments were repeated at least 3 times and the results are expressed as the mean ± SEM. Statistical significance was verified by one-way ANOVA and Tukey's post hoc test. $^{\#\#}$P<0.01 vs. normal, untreated cells; **P<0.01 vs. RANKL-induced cells. GF, *Gleditsiae fructus*; RANKL, receptor activator of nuclear factor-κB ligand; F-actin, filamentous actin.

both the number of TRAP (+) cells and TRAP activity in a dose-dependent manner (Fig. 1B-D).

GF suppresses RANKL-induced bone resorption and F-actin formation. To investigate the impact of GF on osteoclastogenesis and bone resorption, experiments on F-actin ring and pit formation were conducted. The results, as illustrated in Fig. 2A and C, showed that RANKL-treated cells had a higher pit area compared with the untreated cells and GF dose-dependently decreased the pit area. Furthermore, RANKL-treated cells displayed more F-actin rings than the untreated cells, but GF inhibited both the number and structure of F-actin rings, as depicted in Fig. 2B and D.

GF decreases the expression of osteoclastogenesis-related transcription factors. To determine the effect of GF on osteoclastogenesis-related transcription factors, western blotting and RT-PCR were used. As shown in Fig. 3A and B, the RANKL-treated cells exhibited increased expression of NFATc1 compared with the untreated cells. However, GF significantly reduced the protein and mRNA levels of NFATc1 at concentrations of 20 and 40 μg/ml. Furthermore, the results also indicated that treatment with RANKL led to increased protein and mRNA expression levels of c-Fos compared with the untreated cells. Conversely, treatment with 40 μg/ml GF resulted in a decrease in c-Fos protein and mRNA expression levels compared with the untreated cells (Fig. 3C and D).

GF decreases the mRNA expression levels of osteoclast-specific genes. To explore the effects of GF treatment on osteoclast-specific genes, RT-PCR was performed. The results revealed that RANKL-induced cells showed upregulation in the mRNA expression of TRAP (*Acp5*), RANK (*Tnfrsf11a*), MMP-9 (*Mmp9*), CA2 (*Ca2*), osteoclast-associated receptor (OSCAR; *Oscar*), ATP6vod2 (*Atp6v0d2*) and dendritic cell-specific transmembrane protein (DC-STAMP; *Dcstamp*), compared with the non-treated cells (Fig. 4A and B). However, GF treatment (20 and 40 μg/ml) resulted in a decrease in

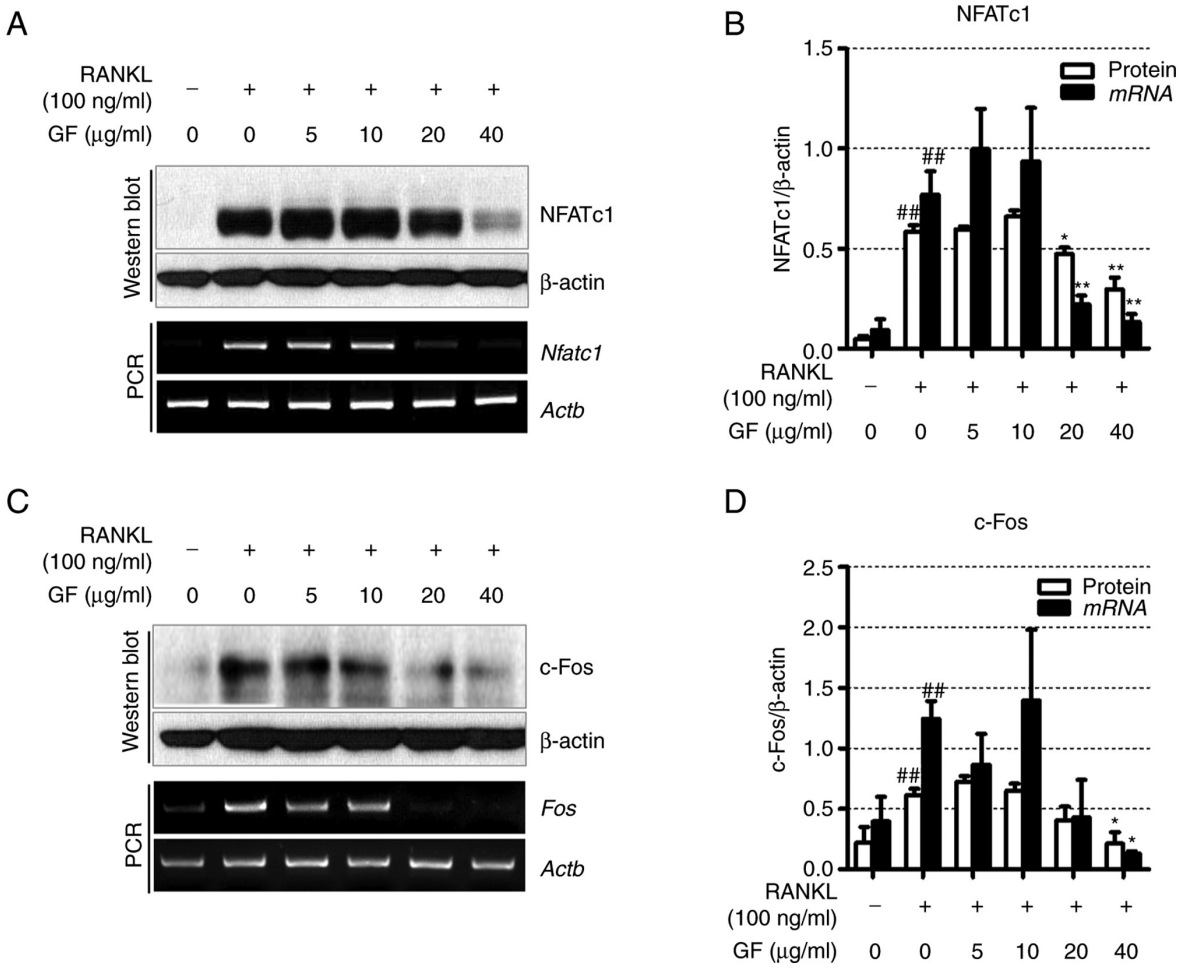

Figure 3. Effect of increasing doses of GF on the expression of NFATc1 and c-Fos. (A) Effect of GF on NFATc1 expression at the protein and mRNA levels was verified by western blotting and RT-PCR. (B) Quantification of NFATc1expression, normalized to β-actin (*Actb*). (C) Effect of GF on c-Fos expression at the protein and mRNA levels was verified by western blotting and RT-PCR. (D) Quantification of c-Fos expression, normalized to β-actin (*Actb*). All experiments were repeated at least 3 times and the results are expressed as the mean ± SEM. Statistical significance was verified by one-way ANOVA and Tukey's post hoc test. $^{##}$P<0.01 vs. normal, untreated cells; *P<0.05 and **P<0.01 vs. RANKL-induced cells. GF, *Gleditsiae fructus*; RANKL, receptor activator of nuclear factor-κB ligand; NFATc1, nuclear factor of activated T cells 1; *Actb*, β-actin; RT-PCR, reverse transcription-PCR.

the mRNA expression of TRAP, RANK, MMP-9, CA2, OSCAR, ATP6vod2 and DC-STAMP, compared with the RANKL-treated cells.

GF does not significantly affect the weight of postmenopausal osteoporotic rats and has a beneficial impact on changes in bone metabolism markers in serum. To further demonstrate the suppressive effect of GF on osteoclast differentiation, formation and bone resorption, an OVX-induced rat model was used. As shown in Fig. 5A, compared with the sham group, the OVX group showed a significant increase in body weight from 3 weeks. The ALN and GF groups did not show significant changes in body weight compared with the OVX group. Uterine weight was significantly reduced in the OVX group compared with the sham group (Fig. 5B). In the E_2 and ALN groups, there was a significant increase in uterine weight compared with that of the OVX group. However, the GF groups showed no changes in uterine weight compared with the sham group.

Next, serum analysis was performed to confirm the effect of GF on bone formation and bone resorption markers. Compared with the sham group, the OVX group exhibited a slight increase in TRAP activity (not significant), as indicated in Fig. 5C. The E_2 and GF-L groups demonstrated a reduction in TRAP activity compared with the OVX group, but this difference was not significant. The ALN group had no significant change in TRAP activity. In the GF-H group, TRAP activity was significantly decreased compared with that in the OVX group. In addition, the ALP level increased in the OVX group compared with the sham group, although the difference was not statistically significant (Fig. 5D). The E_2 group did not show a significant change in ALP levels, while the ALN and GF-L groups demonstrated lower ALP levels compared with the OVX group, although this difference was not statistically significant. The ALP level significantly decreased in the GF-H group compared with the OVX group.

To evaluate the potential impact of GF administration on hepatotoxicity, an analysis of serum AST and ALT levels was conducted. Both factors showed no difference between the SHAM and OVX groups. The E_2 group showed no change in AST levels compared with OVX group and the ALN and GF-L groups appeared to have decreased AST levels compared with the OVX group, but these differences were not significant (Fig. 5E). However, AST levels were significantly decreased in

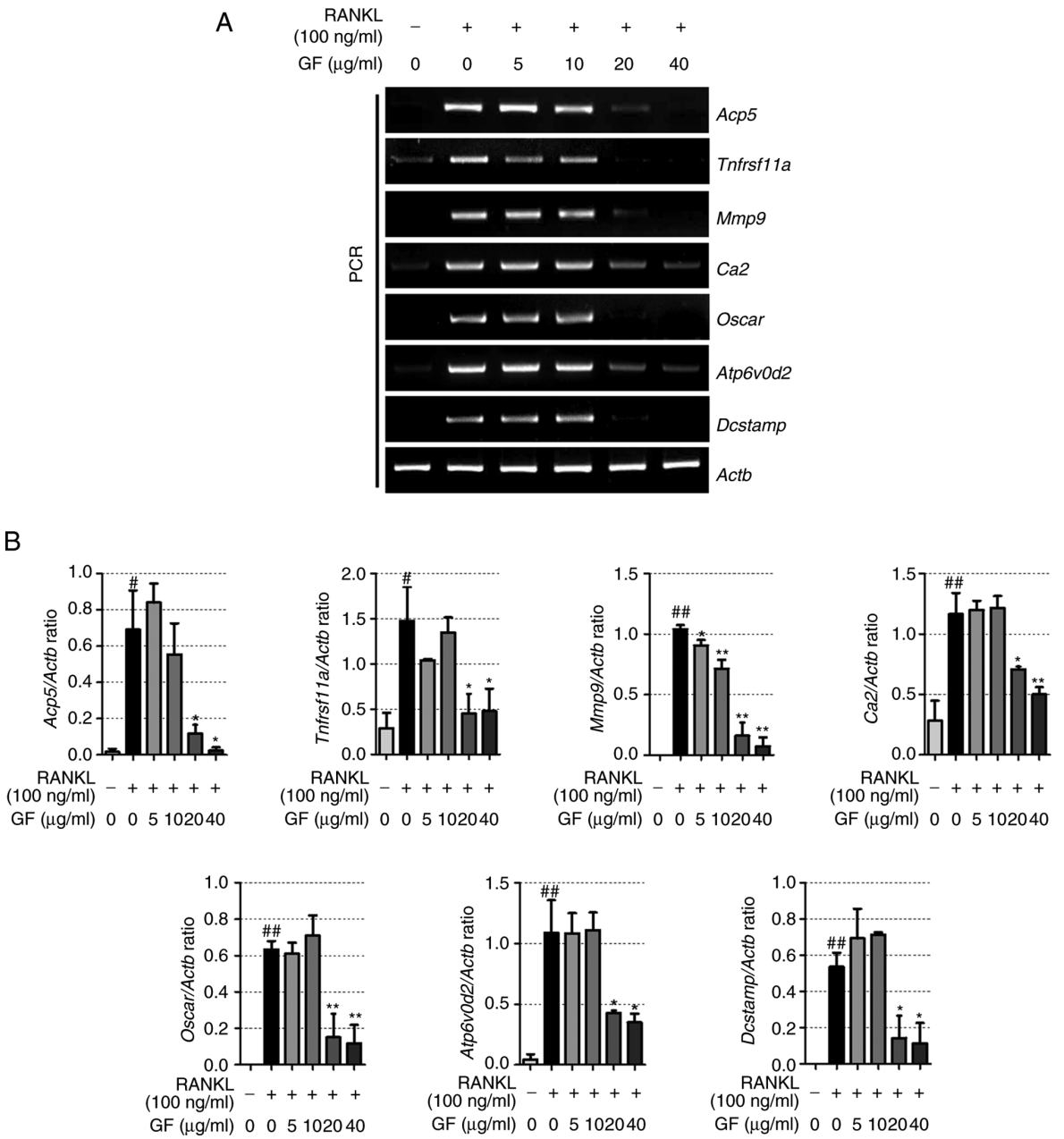

Figure 4. Effect of increasing doses of GF on the expression of genes related to osteoclastogenesis. (A) mRNA expression of TRAP (*Acp5*), RANK (*Tnfrsf11a*), MMP-9 (*Mmp9*), CA2 (*Ca2*), OSCAR (*Oscar*), ATP6v0d2 (*Atp6vod2*) and DC-STAMP (*Dcstamp*) was verified by reverse transcription-PCR. (B) Quantification of the expression of each gene, standardized to β-actin. The experiment was repeated at least 3 times, the results are expressed as the mean ± SEM. Statistical significance was verified by one-way ANOVA and Tukey's post hoc test. $^{\#}$P<0.05 and $^{\#\#}$P<0.01 vs. normal, untreated cells; *P<0.05 and **P<0.01 vs. RANKL-induced cells. GF, *Gleditsiae fructus*; RANKL, receptor activator of nuclear factor-κB ligand; TRAP, tartrate-resistant acid phosphatase; RANK, receptor activator of nuclear factor-κB; MMP-9, matrix metalloproteinase-9; CA2, carbonic anhydrase type II; OSCAR, osteoclast associated Ig-like receptor; ATP6v0d2, ATPase H+ transporting V0 subunit d2; DC-STAMP, dendritic cell-specific transmembrane protein; Actb, β-actin.

the GF-H group compared with the OVX group. In the case of ALT, there were no significant differences between the OVX and drug administered groups (Fig. 5F).

GF inhibits the decrease in bone density and bone micro-structure. To further confirm the *in vitro* results, the ability of GF to inhibit postmenopausal osteoporosis caused by OVX induction was investigated. The OVX models were divided into six groups of 8 rats: sham, OVX, OVX + E_2, OVX + ALN, OVX + GF-L and OVX + GF-H. The impact of GF on bone loss was evaluated using bone microstructure and micro-CT. As shown in the 3D images in Fig. 6A, the OVX group had a decreased BMD relative to the sham group, while the E_2, ALN and GF treatments substantially increased the BMD of the femur, compared with the OVX group. Compared with the sham group, the OVX group exhibited decreased BV/TV and Tb.Th values in the femur, while the E_2, ALN and GF groups demonstrated significant increases in both values, compared with the OVX group; notably, for Tb.Th, there was no significant difference between the GF-L and OVX groups. Additionally, OVX led to increased Tb.Sp in the femur compared with the sham group, while

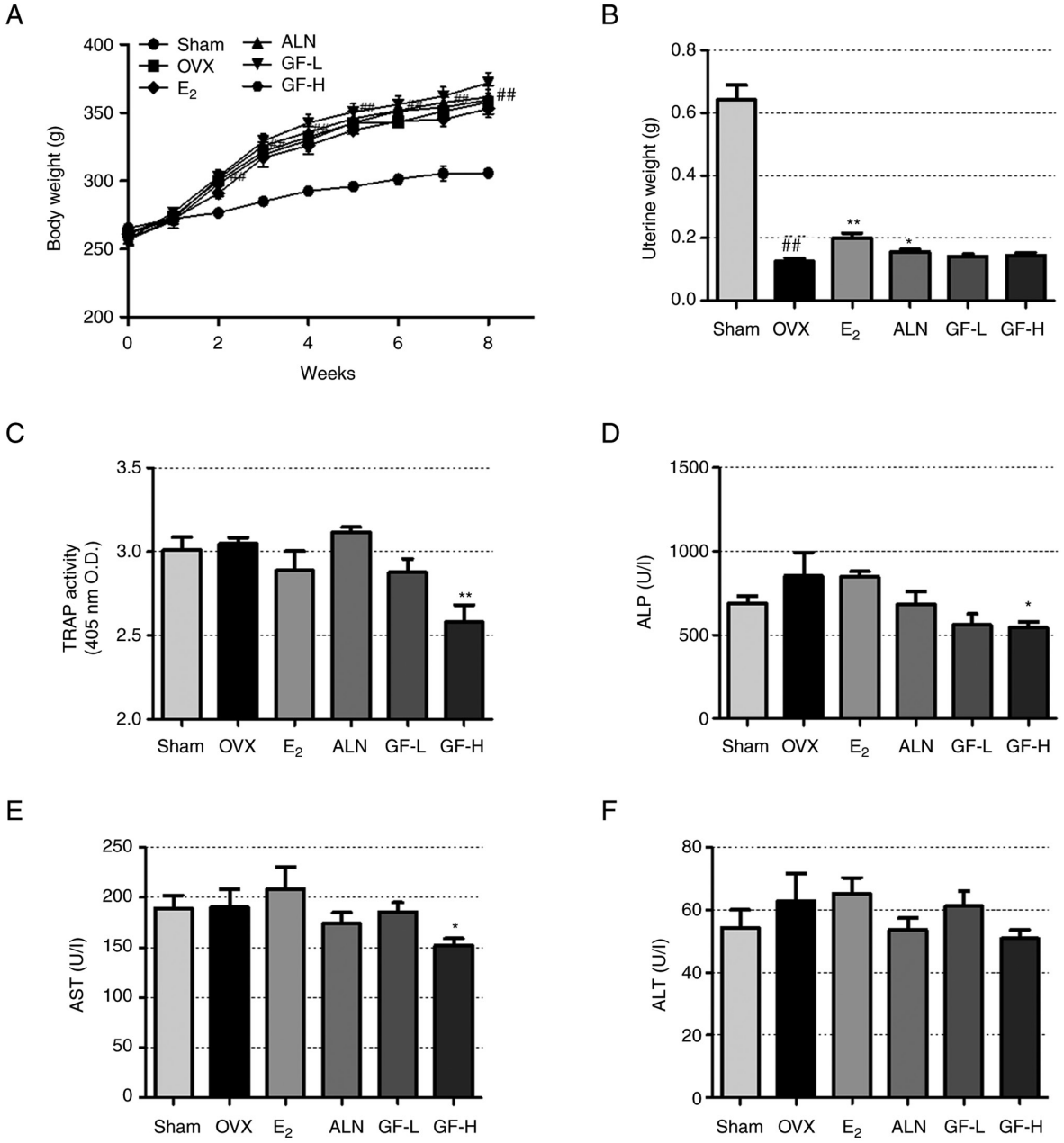

Figure 5. Effect of GF, E_2 and ALN in the rat model of postmenopausal osteoporosis. (A) Animal body weights were measured weekly and (B) uterine weights were measured on the day of sacrifice. (C) TRAP activity, and (D) ALP, (E) AST and (F) ALT levels in serum. The results are expressed as the mean ± SEM (n=8). Statistical significance was verified by one-way ANOVA and Tukey's post hoc test. ##P<0.01 vs. the sham group; *P<0.05 and **P<0.01 vs. the OVX group. GF, *Gleditsiae fructus*; OVX, ovariectomy (rats); TRAP, tartrate-resistant acid phosphatase; ALP, alkaline phosphatase; AST, aspartate aminotransferase; ALT, alanine transaminase; E_2, 17β-estradiol; ALN, alendronate; GF-L, 16.9 mg/kg GF; GF-H, 108.16 mg/kg GF; O.D., optical density.

treatment with E_2, ALN and GF resulted in a decrease in Tb.Sp (Fig. 6B-E).

GF increases the trabecular area and decreases the expression of CTK and NFATc1. To investigate the trabecular area, the expression of NFATc1 and CTK using H&E and IHC staining was examined. IHC staining demonstrated that the levels of NFATc1 and CTK were significantly increased in the OVX group compared with the sham group, and reduced in the E_2, ALN and GF groups compared with the OVX group (Fig. 7A-D). Next, to evaluate the effect of GF on the trabecular area in the femur, H&E staining was performed (Fig. 7E and F). The OVX group displayed a reduction in trabecular area compared with the sham group. However, the E_2, ALN and GF groups showed an increase in trabecular area relative to the OVX group.

GF has no significant effect on osteoblast differentiation. To assess the impact of GF on osteoblasts and the formation of calcified nodules, alizarin red S staining was performed. According to the results depicted in Fig. 8A, GF did not induce a notable effect on the osteoblast differentiation induced by A.A and B.G.P. Additionally, assessment of the extracted dye showed that GF did not demonstrate a higher absorbance than the control (Fig. 8B). Furthermore, the tested concentration of GF did not exhibit any cytotoxicity (Fig. 8C).

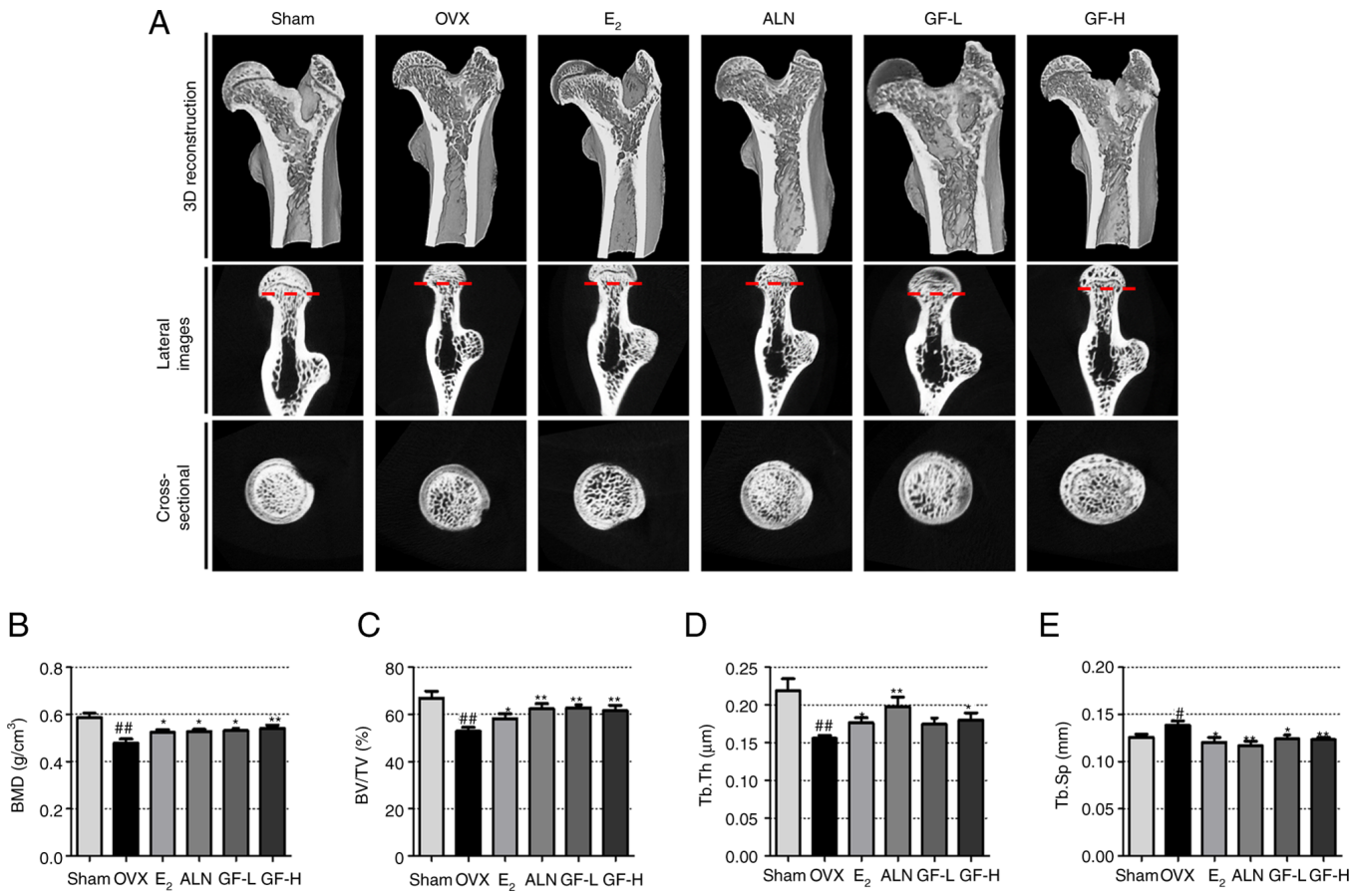

Figure 6. Effect of GF, E_2 and ALN on changes in bone density and bone microstructure of the femoral head. (A) Images of the femur were captured using micro-CT. Bone microstructure factors, (B) BMD, (C) BV/TV, (D) Tb.Th and (E) Tb.Sp were measured using SkyScan software. The results are expressed as the mean ± SEM (n=8). Statistical significance was verified by one-way ANOVA and Tukey's post hoc test. $^{\#}$P<0.05 and $^{\#\#}$P<0.01 vs. the sham group; *P<0.05 and **P<0.01 vs. the OVX group. GF, *Gleditsiae fructus*; OVX, ovariectomy (rats); micro-CT, microcomputed tomography; BV/TV, bone volume/total volume; Tb.Th, trabecular thickness; Tb.Sp, trabecular separation; E_2, 17β-estradiol; ALN, alendronate; GF-L, 16.9 mg/kg GF; GF-H, 108.16 mg/kg GF.

Quantitative analysis of GF. Echinocystic acid and oleanolic acid are active ingredients of GF (20). Chromatographic peaks of standard echinocystic acid and oleanolic acid ingredients were detected (Fig. 9A) for the comparison with GF (Fig. 9B). It was demonstrated that peaks for both chromatograms were detected at the same time, and the contents of echinocystic acid and oleanolic acid in GF were confirmed to be 8.97 and 10.8 mg/g, respectively.

Discussion

The present study indicated that GF inhibited osteoclastogenesis and the expression of osteoclastogenesis-related markers. In particular, GF decreased bone loss in the OVX-induced rat models. Notably, GF had a protective effect on bone structure in the OVX-induced rats similar to that of E_2 and ALN, despite the absence of estrogen-like activity. These results suggest that GF could be used as an alternative therapy to prevent and treat bone loss.

Botanical drugs, derived from natural sources, offer several advantages for osteoporosis treatment, including their natural origin, lower risk of side effects, their ability to act on multiple pathways in the body and their increasing popularity in the expanding natural products market. Additionally, botanical drugs are often less expensive to develop and manufacture, can be administered orally and may improve patient compliance. As research continues, more effective and targeted botanical drugs may be developed, with the potential to significantly improve the lives of patients with osteoporosis (31-34).

RAW 264.7 cells are a suitable model for studying osteoclast formation and function, as the cells readily differentiate into osteoclasts upon exposure to RANKL (35). TRAP has long been used as a histochemical marker for osteoclasts (36). In the present study, GF substantially decreased the number of TRAP (+) cells and TRAP activity. In order to evaluate the bone resorption ability of osteoclasts, researchers typically use the pit formation assay (37). In the present study, it was observed that the pit area was reduced by GF treatment compared with the control group, indicating inhibition of bone resorption. Upon osteoclast attachment to bone, osteoclasts produce F-actin structures and, in this sealing area, a corrugated border of osteoclasts is formed (38). In the present study, GF decreased the production of F-actin rings compared with that of the control group. The results showed that GF has an anti-osteoporotic effect by inhibiting osteoclastogenesis and bone resorption.

RANKL and RANK are factors that play a key role in osteoclastogenesis and activation. RANK is mainly expressed in osteoclast progenitor cells derived from hematopoietic stem cells and RANKL is mainly expressed in osteoblasts

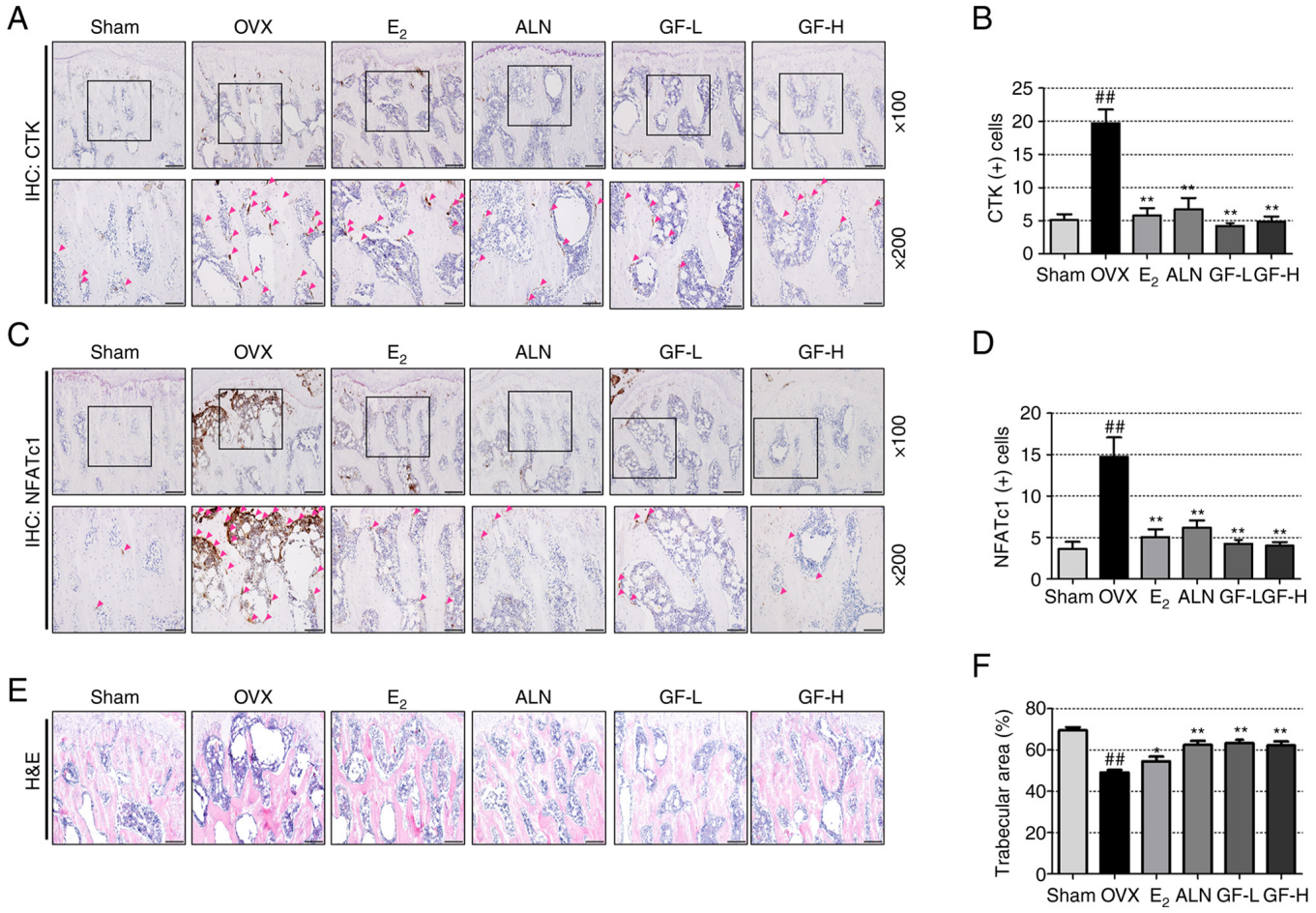

Figure 7. Effect of GF, E_2 and ALN on histochemical and histological changes in the femoral head. (A) CTK (+) cells in the femoral ball head (red arrow) were detected by IHC staining. (B) The number of CTK (+) cells was determined using ImageJ software. (C) NFATc1 (+) cells in the femoral ball head (red arrow) were detected by IHC staining. (D) The number of NFATc1 (+) cells was determined using ImageJ software. (E) The histological changes of the femur were analyzed by H&E staining (magnification: x100; scale bar, 100 μm). (F) The area of the trabecular bone was measured using ImageJ. The results are expressed as the mean ± SEM (n=8). Statistical significance was verified by one-way ANOVA and Tukey's post hoc test. $^{##}$P<0.01 vs. the sham group; *P<0.05 and **P<0.01 vs. the OVX group. GF, *Gleditsiae fructus*; OVX, ovariectomy (rats); IHC, immunohistochemistry; CTK, cathepsin K; NFATc1, nuclear factor of activated T cells 1; H&E, hematoxylin and eosin; E_2, 17β-estradiol; ALN, alendronate; GF-L, 16.9 mg/kg GF; GF-H, 108.16 mg/kg GF.

derived from stromal cells (39). RANK knockout mice exhibit severe osteopetrosis due to an apparent blockade of osteoclastogenesis (40). Upon RANKL and RANK binding, osteoclastogenesis-related transcription factors, such as NFATc1 and c-Fos, are expressed to regulate the expression of osteoclast-specific genes (41,42). NFATc1 is a member of the nuclear factor of activated T cells family. According to previous studies, embryonic stem cells deficient in NFATc1 cannot differentiate into osteoclasts (17,43). c-Fos is a member of the Fos family and plays an essential role in the differentiation of macrophages into osteoclasts (44). A previous study has shown that mice deficient in c-Fos develop osteopetrosis due to a lack of osteoclast formation (45). In the present study, western blotting and RT-PCR data revealed that NFATc1 and c-Fos levels were significantly downregulated by GF treatment. Based on these data, GF has an anti-osteoporotic effect by suppressing the expression of NFATc1 and c-Fos signaling pathways.

Upon activation of NFATc1, specific genes related to osteoclastogenesis are activated and are abundantly expressed in osteoclasts (17). TRAP is known to be an important cytochemical marker of osteoclasts. The serum concentration of TRAP has been used as a phenotype indicator of bone resorption and osteoclast function (46), and osteoclasts isolated from TRAP knockout animals showed a cellular intrinsic defect in bone resorption (47). In addition, mice lacking TRAP had an osteopetrotic bone phenotype at 4 weeks of age (48). MMP-9 is a bone resorbing factor and expression of this molecule in early osteoclasts induces transformation into mature osteoclasts (49). Mice deficient in MMP-9 exhibited an accumulation of late hypertrophic chondrocytes (49). A previous study has shown that mice with null mutations in MMP-9 exhibited abnormal patterns of skeletal growth plate ossification and vascularization (50). CA2 acts as a mediator of hormones that stimulate bone resorption and osteoclast formation and is detected in the early stages of osteoclast differentiation (51,52). Individuals with a deficiency in CA2 have reduced bone resorption and clinical osteopetrosis (53). Furthermore, *in vivo*, CA2-deficient mice have a human-like phenotype with the same genetic enzymatic deletion (53). OSCAR has been reported to be involved in cell-cell interactions between osteoblasts and osteoclasts and is expressed at a later stage of osteoclast maturation in mice (54,55). ATP6v0d2 acts as a regulatory element of cell fusion in osteoclastogenesis and is an essential component of

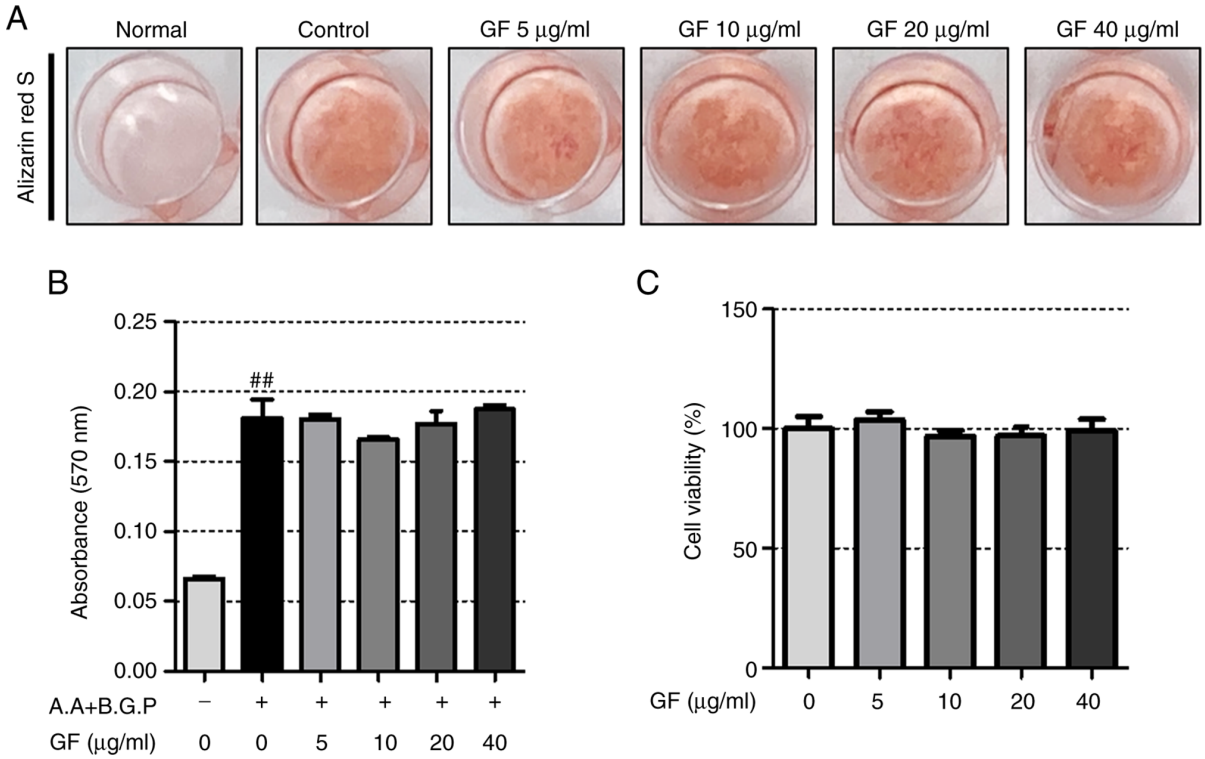

Figure 8. Effect of increasing doses of GF on the osteogenesis effect in MC3T3-E1 cells. (A) Cells were stained with alizarin red S. (B) The level of extracted alizarin red S dye was measured. (C) Cell viability was determined using the Cell Counting Kit-8 assay. The experiments were repeated at least 3 times and the results are expressed as the mean ± SEM. Statistical significance was verified by one-way ANOVA and Tukey's post hoc test. $^{##}P<0.01$ vs. untreated cells. A.A, ascorbic acid; B.G.P, β-glycerol phosphate; GF, *Gleditsiae fructus*.

osteoclast-specific proton pumps that mediate extracellular acidification in bone resorption (56). The differentiation of osteoclasts and osteoblasts is regulated by DC-STAMP, which is a crucial factor in maintaining bone homeostasis (57). Osteoclast formation is dependent on cell-cell fusion, which is facilitated by Atp6vod2 and DC-STAMP with mice deficient in these factors developing osteopetrosis due to the absence of osteoclasts (58,59). The results of the present study also demonstrated that GF treatment decreased the expression of osteoclast-specific genes (*Acp5, Tnfrsf11a, Mmp9, Ca2, Oscar, Atp6v0d2 and Dcstamp*). This indicated that GF could regulate the NFATc1/c-Fos signaling pathway, thereby suppressing the expression of osteoclast-specific genes.

Bone is maintained by the harmonious and balanced activity of osteoclasts and osteoblasts. However, when the balance is disturbed due to excessive activity of osteoclasts, bone diseases such as osteoporosis occur (15). OVX causes bone loss due to estrogen deficiency in OVX rat models. This effect is similar to the change that occurs in humans and is widely used in experiments investigating osteoporosis (6,60). Estrogen prevents weight gain by regulating food intake and behavior. In addition, ablated ovaries cause functional loss of the uterus, reducing its weight and volume. Weight gain is a common symptom observed in the OVX-induced model. Decreased uterine weight also demonstrates the successful establishment of the OVX-induced model (60). In the present study, after 3 weeks, a significant increase in body weight was observed in the OVX group compared with the sham group. There was no change in body weight in the ALN, E_2, GF-L and GF-H groups compared with the OVX group. According to the experimental results, the OVX-induced model was successfully established. Furthermore, OVX induced a substantial decrease in uterine weight, thereby validating the successful establishment of a menopausal-like model. Both the positive control groups, E_2 and ALN, countered this reduction, whereas the GF group did not demonstrate any significant effect.

TRAP is utilized as a serum marker to confirm the anti-osteoporotic effects in both animal experiments and an *in vitro* study (61). ALP is a marker expressed in the early stages of osteoblast differentiation (62). Previous studies have shown that the levels of ALP are increased in models of estrogen deficiency (63) and excessive osteoclast activity due to estrogen deficiency also increases osteoblast activity (64). In the present study, both TRAP and ALP markers increased in the OVX group compared with the sham group, but the differences did not reach statistical significance. In a prior study, a significant difference between the two groups was observed after 12 weeks post-OVX, suggesting that the shorter sacrifice period of 8 weeks in the present study may have contributed to the lack of statistical significance (65). Nonetheless, the results of the present study suggested that the GF-H group may serve as an effective osteoclast inhibitor, as it demonstrated a significant inhibition of both markers when compared with the OVX group.

Recent research has shown that microarchitecture is important along with bone density (66), thus, the importance of histomorphometry for evaluation of the bone trabecular structure is receiving attention. Histopathological methods have been traditionally used for bone morphometry (67). However, bone tissue morphometric methods using imaging

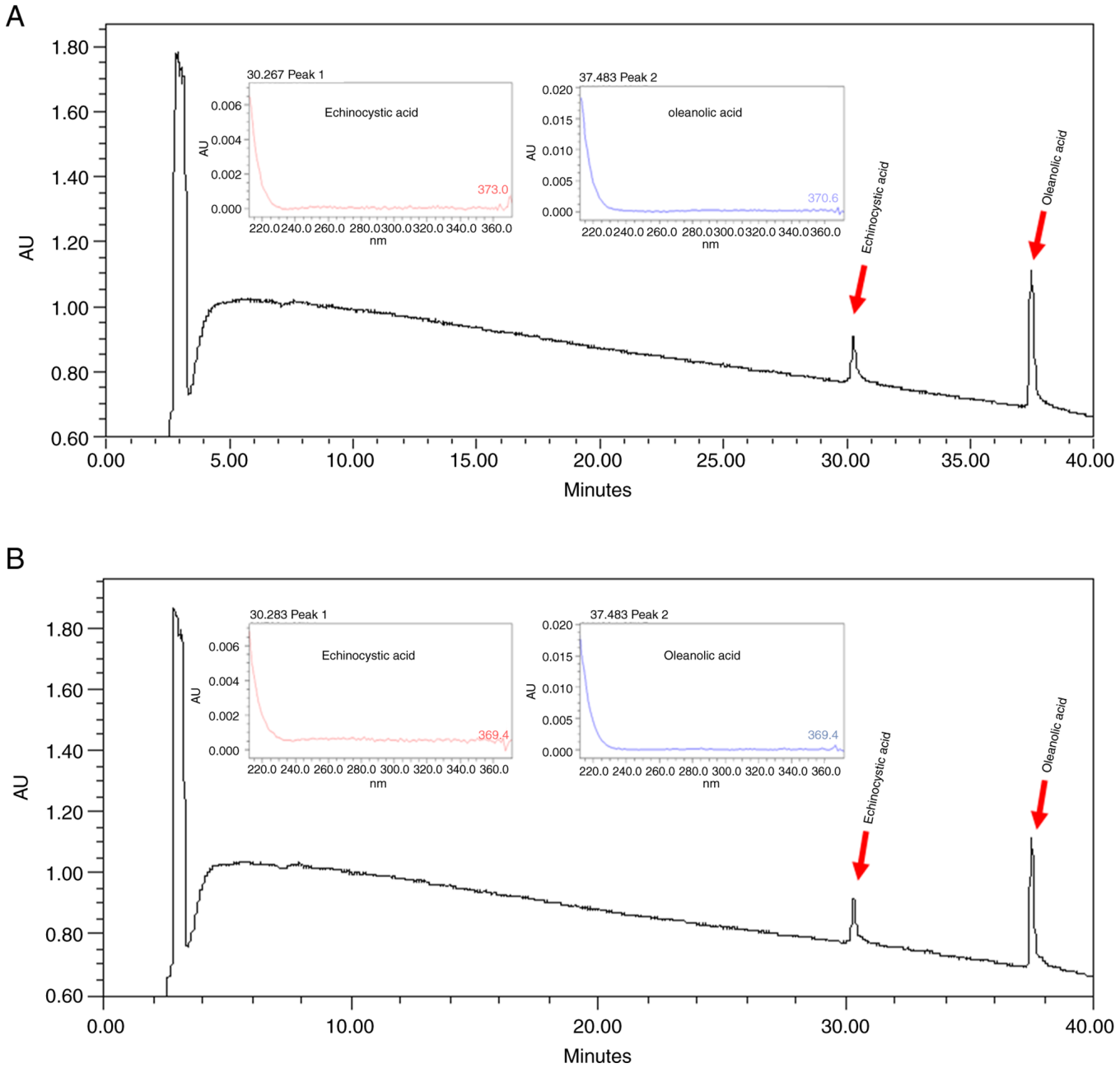

Figure 9. Quantitative analysis of GF using high-performance liquid chromatography analysis. Standard peaks of (A) echinocystic acid and oleanolic acid and (B) GF were detected. AU, absorbance units; GF, *Gleditsiae fructus*.

techniques such as micro-CT and high-resolution MRI have also been actively studied (68). In addition, these methods show an excellent correlation compared with histopathological histomorphometry (69). Micro-CT is high-resolution CT with pixel sizes typically ranging 1-50 μm and X-rays can be used to investigate the microstructure of a sample. Furthermore, micro-CT characterization consists of three main sequential processes: Acquisition, reconstruction and analysis (70,71). Bone density is defined as the amount of bone minerals in bone tissue. It is known that the lower the BMD, the higher the risk of fracture, even from a small impact (72). Tb.Th is a measure of the thickness of numerous spheres in the trabecular column and can be indicative of osteoporosis if a decrease in the bone trabecular thickness is detected. Tb.Sp is the average diameter of the trabecular area and as osteoporosis progresses, the thickness increases (73,74). In the present study, BMD and bone microarchitecture parameters, such as BV/TV and Tb.Th decreased in the OVX group compared with the sham group, and a decrease in the Tb.Sp of the E_2, ANL and GF groups compared with the OVX group was observed. Trabecular bone structural parameters derived from micro-CT data are based on traditional static osseous morphometry that evaluate the thickness, connectivity, distribution and spacing of the trabeculae (75) and the representative method for analyzing trabecular bone is H&E staining (67,76). In the present study, to evaluate morphological changes in bone tissue, H&E staining was used to measure trabecular area while IHC staining was employed to measure osteoclast-related parameters. H&E staining revealed that bone loss was significantly decreased by E_2,

ALN and GF treatment compared with that of the OVX group. Furthermore, compared with the OVX group, femoral bone from rats treated with E_2, ALN and GF exhibited significant reductions in the expression of NFATc1 and CTK. These results showed that GF treatment decreased bone loss induced by OVX.

The limitations of the present study are as follows: i) When RANK-RANKL binds, TRAF6, MAPK and NF-kB are activated. Subsequently, c-Fos and NFATc1 expression is induced (77). Further studies of the effects of GF on MAPK and NF-κB are needed to further evaluate the mechanism of the inhibitory effect of GF on osteoclastogenesis; and ii) in the present study, GF demonstrated a notable inhibition of osteoclast differentiation. However, the specific component within GF that is responsible for this effect remains unclear. Previous research has identified echinocystic acid (78) and oleanolic acid (79), both prominent constituents of GF, as potential contributors to the inhibition of osteoclast differentiation. Nevertheless, to precisely ascertain the osteoclast inhibitory effect of GF, further investigation is warranted, encompassing comprehensive validation of the GF fraction and all its constituent components.

In conclusion, the data from the present study demonstrated that GF plays a protective role in the OVX-induced model of postmenopausal osteoporosis by decreasing osteoclastogenesis, osteoclast formation and bone resorption. Thus, GF has the potential to act as an alternative therapeutic agent for the prevention and treatment of postmenopausal osteoporosis.

Acknowledgements

Not applicable.

Funding

This research was supported by a grant from the Korea Health Technology R&D Project through the Korea Health Industry Development Institute, funded by the Ministry of Health and Welfare, Republic of Korea (grant no. HF21C0092).

Availability of data and materials

All data generated or analyzed during this study are included in this published article.

Authors' contributions

HSJ conceptualized the study; CYC and SHK performed all experiments; MK, BCK, TKK and JHK contributed to the statistical analysis; JHK, YS and HSJ helped interpret the results; CYC and SHK drafted the manuscript. CYC, SHK, BCK, TKK, JHK, MK, YS and HSJ participated in obtaining materials and confirm the authenticity of all the raw data. All authors read and approved the final manuscript.

Ethics approval and consent to participate

All animal experiments were approved by The Kyung Hee University Animal Care and Use Committee (approval no. KHSASP-21-185).

Patient consent for publication

Not applicable.

Competing interests

The authors declare that they have no competing interests.

References

1. Crimmins EM: Lifespan and healthspan: Past, present, and promise. Gerontologist 55: 901-911, 2015.
2. Riggs BL and Melton LJ III: The worldwide problem of osteoporosis: Insights afforded by epidemiology. Bone 17 (5 Suppl): 505S-511S, 1995.
3. Cosman F, de Beur SJ, LeBoff MS, Lewiecki EM, Tanner B, Randall S and Lindsay R; National Osteoporosis Foundation: Clinician's guide to prevention and treatment of osteoporosis. Osteoporos Int 25: 2359-2381, 2014.
4. Matsuo K and Irie N: Osteoclast-osteoblast communication. Arch Biochem Biophys 473: 201-209, 2008.
5. Feng X and McDonald JM: Disorders of bone remodeling. Annu Rev Pathol 6: 121-145, 2011.
6. Sözen T, Özışık L and Başaran NÇ: An overview and management of osteoporosis. Eur J Rheumatol 4: 46-56, 2017.
7. Tella SH and Gallagher JC: Prevention and treatment of postmenopausal osteoporosis. J Steroid Biochem Mol Biol 142: 155-170, 2014.
8. Rasmusson L and Abtahi J: Bisphosphonate associated osteonecrosis of the jaw: An update on pathophysiology, risk factors, and treatment. Int J Dent 2014: 471035, 2014.
9. Abrahamsen B: Bisphosphonate adverse effects, lessons from large databases. Curr Opin Rheumatol 22: 404-409, 2010.
10. Collin-Osdoby P, Yu X, Zheng H and Osdoby P: RANKL-mediated osteoclast formation from murine RAW 264.7 cells. Methods Mol Med 80: 153-166, 2003.
11. Clohisy JC, Frazier E, Hirayama T and Abu-Amer Y: RANKL is an essential cytokine mediator of polymethylmethacrylate particle-induced osteoclastogenesis. J Orthop Res 21: 202-212, 2003.
12. Galibert L, Tometsko ME, Anderson DM, Cosman D and Dougall WC: The involvement of multiple tumor necrosis factor receptor (TNFR)-associated factors in the signaling mechanisms of receptor activator of NF-kappaB, a member of the TNFR superfamily. J Biol Chem 273: 34120-34127, 1998.
13. Kobayashi N, Kadono Y, Naito A, Matsumoto K, Yamamoto T, Tanaka S and Inoue J: Segregation of TRAF6-mediated signaling pathways clarifies its role in osteoclastogenesis. EMBO J 20: 1271-1280, 2001.
14. Teitelbaum SL: Bone resorption by osteoclasts. Science 289: 1504-1508, 2000.
15. Boyle WJ, Simonet WS and Lacey DL: Osteoclast differentiation and activation. Nature 423: 337-342, 2003.
16. Takayanagi H, Kim S, Koga T, Nishina H, Isshiki M, Yoshida H, Saiura A, Isobe M, Yokochi T, Inoue J, *et al*: Induction and activation of the transcription factor NFATc1 (NFAT2) integrate RANKL signaling in terminal differentiation of osteoclasts. Dev Cell 3: 889-901, 2002.
17. Kim JH and Kim N: Regulation of NFATc1 in osteoclast differentiation. J Bone Metab 21: 233-241, 2014.
18. Lai P, Du JR, Zhang MX, Kuang X, Li YJ, Chen YS and He Y: Aqueous extract of Gleditsia sinensis Lam. Fruits improves serum and liver lipid profiles and attenuates atherosclerosis in rabbits fed a high-fat diet. J Ethnopharmacol 137: 1061-1066, 2011.
19. Güçlü-Ustündağ O and Mazza G: Saponins: Properties, applications and processing. Crit Rev Food Sci Nutr 47: 231-258, 2007.
20. Chen J, Li Z, Zheng KY, Guo AJ, Zhu KY, Zhang WL, Zhan JY, Dong TT, Su Z and Tsim KW: Chemical fingerprinting and quantitative analysis of two common Gleditsia sinensis fruits using HPLC-DAD. Acta Pharm 63: 505-515, 2013.
21. Joh EH, Gu W and Kim DH: Echinocystic acid ameliorates lung inflammation in mice and alveolar macrophages by inhibiting the binding of LPS to TLR4 in NF-κB and MAPK pathways. Biochem Pharmacol 84: 331-340, 2012.

22. Hyam SR, Jang SE, Jeong JJ, Joh EH, Han MJ and Kim DH: Echinocystic acid, a metabolite of lancemaside A, inhibits TNBS-induced colitis in mice. Int Immunopharmacol 15: 433-441, 2013.
23. Lee W, Yang EJ, Ku SK, Song KS and Bae JS: Anti-inflammatory effects of oleanolic acid on LPS-induced inflammation in vitro and in vivo. Inflammation 36: 94-102, 2013.
24. Choi JK, Oh HM, Lee S, Park JW, Khang D, Lee SW, Lee WS, Rho MC and Kim SH: Oleanolic acid acetate inhibits atopic dermatitis and allergic contact dermatitis in a murine model. Toxicol Appl Pharmacol 269: 72-80, 2013.
25. Kim JY, Cheon YH, Oh HM, Rho MC, Erkhembaatar M, Kim MS, Lee CH, Kim JJ, Choi MK, Yoon KH, *et al*: Oleanolic acid acetate inhibits osteoclast differentiation by downregulating PLCγ2-Ca(2+)-NFATc1 signaling, and suppresses bone loss in mice. Bone 60: 104-111, 2014.
26. Lacativa PG and Farias ML: Osteoporosis and inflammation. Arq Bras Endocrinol Metabol 54: 123-132, 2010.
27. Lee S, Kim M, Hong S, Kim EJ, Kim JH, Sohn Y and Jung HS: Effects of sparganii rhizoma on osteoclast formation and osteoblast differentiation and on an OVX-induced bone loss model. Front Pharmacol 12: 797892, 2022.
28. Tschöp MH, Speakman JR, Arch JR, Auwerx J, Brüning JC, Chan L, Eckel RH, Farese RV Jr, Galgani JE, Hambly C, *et al*: A guide to analysis of mouse energy metabolism. Nat Methods 9: 57-63, 2011.
29. Wang Y, Huang P, Tang PF, Chan KM and Li G: Alendronate (ALN) combined with osteoprotegerin (OPG) significantly improves mechanical properties of long bone than the single use of ALN or OPG in the ovariectomized rats. J Orthop Surg Res 6: 34, 2011.
30. Beeton C, Garcia A and Chandy KG: Drawing blood from rats through the saphenous vein and by cardiac puncture. J Vis Exp: 266, 2007.
31. Dietz BM, Hajirahimkhan A, Dunlap TL and Bolton JL: Botanicals and their bioactive phytochemicals for women's health. Pharmacol Rev 68: 1026-1073, 2016.
32. He J, Li X, Wang Z, Bennett S, Chen K, Xiao Z, Zhan J, Chen S, Hou Y, Chen J, *et al*: Therapeutic anabolic and anticatabolic benefits of natural Chinese medicines for the treatment of osteoporosis. Front Pharmacol 10: 1344, 2019.
33. Słupski W, Jawień P and Nowak B: Botanicals in postmenopausal osteoporosis. Nutrients 13: 1609, 2021.
34. Wang T, Liu Q, Tjhioe W, Zhao J, Lu A, Zhang G, Tan RX, Zhou M, Xu J and Feng HT: Therapeutic potential and outlook of alternative medicine for osteoporosis. Curr Drug Targets 18: 1051-1068, 2017.
35. Hartley JW, Evans LH, Green KY, Naghashfar Z, Macias AR, Zerfas PM and Ward JM: Expression of infectious murine leukemia viruses by RAW264.7 cells, a potential complication for studies with a widely used mouse macrophage cell line. Retrovirology 5: 1, 2008.
36. Vincent C, Kogawa M, Findlay DM and Atkins GJ: The generation of osteoclasts from RAW 264.7 precursors in defined, serum-free conditions. J Bone Miner Metab 27: 114-119, 2009.
37. Vesprey A and Yang W: Pit assay to measure the bone resorptive activity of bone marrow-derived osteoclasts. Bio Protoc 6: e1836, 2016.
38. Matsubara T, Kinbara M, Maeda T, Yoshizawa M, Kokabu S and Takano Yamamoto T: Regulation of osteoclast differentiation and actin ring formation by the cytolinker protein plectin. Biochem Biophys Res Commun 489: 472-476, 2017.
39. Boyce BF and Xing L: Functions of RANKL/RANK/OPG in bone modeling and remodeling. Arch Biochem Biophys 473: 139-146, 2008.
40. Dougall WC, Glaccum M, Charrier K, Rohrbach K, Brasel K, De Smedt T, Daro E, Smith J, Tometsko ME, Maliszewski CR, *et al*: RANK is essential for osteoclast and lymph node development. Genes Dev 13: 2412-2424, 1999.
41. Yamashita T, Yao Z, Li F, Zhang Q, Badell IR, Schwarz EM, Takeshita S, Wagner EF, Noda M, Matsuo K, *et al*: NF-kappaB p50 and p52 regulate receptor activator of NF-kappaB ligand (RANKL) and tumor necrosis factor-induced osteoclast precursor differentiation by activating c-Fos and NFATc1. J Biol Chem 282: 18245-18253, 2007.
42. Fujioka S, Niu J, Schmidt C, Sclabas GM, Peng B, Uwagawa T, Li Z, Evans DB, Abbruzzese JL and Chiao PJ: NF-kappaB and AP-1 connection: Mechanism of NF-kappaB-dependent regulation of AP-1 activity. Mol Cell Biol 24: 7806-7819, 2004.
43. Asagiri M, Sato K, Usami T, Ochi S, Nishina H, Yoshida H, Morita I, Wagner EF, Mak TW, Serfling E and Takayanagi H: Autoamplification of NFATc1 expression determines its essential role in bone homeostasis. J Exp Med 202: 1261-1269, 2005.
44. Grigoriadis AE, Wang ZQ, Cecchini MG, Hofstetter W, Felix R, Fleisch HA and Wagner EF: c-Fos: A key regulator of osteoclast-macrophage lineage determination and bone remodeling. Science 266: 443-448, 1994.
45. Arai A, Mizoguchi T, Harada S, Kobayashi Y, Nakamichi Y, Yasuda H, Penninger JM, Yamada K, Udagawa N and Takahashi N: Fos plays an essential role in the upregulation of RANK expression in osteoclast precursors within the bone microenvironment. J Cell Sci 125: 2910-2917, 2012.
46. Ballanti P, Minisola S, Pacitti MT, Scarnecchia L, Rosso R, Mazzuoli GF and Bonucci E: Tartrate-resistant acid phosphate activity as osteoclastic marker: Sensitivity of cytochemical assessment and serum assay in comparison with standardized osteoclast histomorphometry. Osteoporos Int 7: 39-43, 1997.
47. Bune AJ, Hayman AR, Evans MJ and Cox TM: Mice lacking tartrate-resistant acid phosphatase (Acp 5) have disordered macrophage inflammatory responses and reduced clearance of the pathogen, Staphylococcus aureus. Immunology 102: 103-113, 2001.
48. Blumer MJ, Hausott B, Schwarzer C, Hayman AR, Stempel J and Fritsch H: Role of tartrate-resistant acid phosphatase (TRAP) in long bone development. Mech Dev 129: 162-176, 2012.
49. Ortega N, Behonick DJ, Colnot C, Cooper DNW and Werb Z: Galectin-3 is a downstream regulator of matrix metalloproteinase-9 function during endochondral bone formation. Mol Biol Cell 16: 3028-3039, 2005.
50. Vu TH, Shipley JM, Bergers G, Berger JE, Helms JA, Hanahan D, Shapiro SD, Senior RM and Werb Z: MMP-9/gelatinase B is a key regulator of growth plate angiogenesis and apoptosis of hypertrophic chondrocytes. Cell 93: 411-422, 1998.
51. David JP, Rincon M, Neff L, Horne WC and Baron R: Carbonic anhydrase II is an AP-1 target gene in osteoclasts. J Cell Physiol 188: 89-97, 2001.
52. Negishi-Koga T and Takayanagi H: Ca2+-NFATc1 signaling is an essential axis of osteoclast differentiation. Immunol Rev 231: 241-256, 2009.
53. Alsharidi A, Al-Hamed M and Alsuwaida A: Carbonic anhydrase II deficiency: Report of a novel mutation. CEN Case Rep 5: 108-112, 2016.
54. Nedeva IR, Vitale M, Elson A, Hoyland JA and Bella J: Role of OSCAR signaling in osteoclastogenesis and bone disease. Front Cell Dev Biol 9: 641162, 2021.
55. Nemeth K, Schoppet M, Al-Fakhri N, Helas S, Jessberger R, Hofbauer LC and Goettsch C: The role of osteoclast-associated receptor in osteoimmunology. J Immunol 186: 13-18, 2011.
56. Wu H, Xu G and Li YP: Atp6v0d2 is an essential component of the osteoclast-specific proton pump that mediates extracellular acidification in bone resorption. J Bone Miner Res 24: 871-885, 2009.
57. Chiu YH and Ritchlin CT: DC-STAMP: A key regulator in osteoclast differentiation. J Cell Physiol 231: 2402-2407, 2016.
58. Yagi M, Miyamoto T, Sawatani Y, Iwamoto K, Hosogane N, Fujita N, Morita K, Ninomiya K, Suzuki T, Miyamoto K, *et al*: DC-STAMP is essential for cell-cell fusion in osteoclasts and foreign body giant cells. J Exp Med 202: 345-351, 2005.
59. Lee SH, Rho J, Jeong D, Sul JY, Kim T, Kim N, Kang JS, Miyamoto T, Suda T, Lee SK, *et al*: v-ATPase V0 subunit d2-deficient mice exhibit impaired osteoclast fusion and increased bone formation. Nat Med 12: 1403-1409, 2006.
60. Kalu DN: The ovariectomized rat model of postmenopausal bone loss. Bone Miner 15: 175-191, 1991.
61. Kim M, Kim JH, Hong S, Kwon B, Kim EY, Jung HS and Sohn Y: Effects of melandrium firmum rohrbach on RANKL-induced osteoclast differentiation and OVX rats. Mol Med Rep 24: 610, 2021.
62. Seibel MJ: Biochemical markers of bone turnover: Part I: Biochemistry and variability. Clin Biochem Rev 26: 97-122, 2005.
63. Kuo TR and Chen CH: Bone biomarker for the clinical assessment of osteoporosis: Recent developments and future perspectives. Biomark Res 5: 18, 2017.
64. Väänänen HK and Härkönen PL: Estrogen and bone metabolism. Maturitas 23 (Suppl): S65-S69, 1996.
65. Tantikanlayaporn D, Wichit P, Weerachayaphorn J, Chairoungdua A, Chuncharunee A, Suksamrarn A and Piyachaturawat P: Bone sparing effect of a novel phytoestrogen diarylheptanoid from Curcuma comosa Roxb. In ovariectomized rats. PLoS One 8: e78739, 2013.
66. Wagner PP, Whittier DE, Foesser D, Boyd SK, Chapurlat R and Szulc P: Bone microarchitecture decline and risk of fall and fracture in men with poor physical performance-the STRAMBO study. J Clin Endocrinol Metab 106: e5180-e5194, 2021.

67. Osterhoff G, Morgan EF, Shefelbine SJ, Karim L, McNamara LM and Augat P: Bone mechanical properties and changes with osteoporosis. Injury 47 (Suppl 2): S11-S20, 2016.
68. Czeibert K, Baksa G, Grimm A, Nagy SA, Kubinyi E and Petneházy Ö: MRI, CT and high resolution macro-anatomical images with cryosectioning of a Beagle brain: Creating the base of a multimodal imaging atlas. PLoS One 14: e0213458, 2019.
69. Lasbleiz J, Burgun A, Marin F, Rolland Y and Duvauferrier R: Vertebral trabecular network analysis on CT images. J Radiol 86: 645-649, 2005 (In French).
70. Cortet B, Chappard D, Boutry N, Dubois P, Cotten A and Marchandise X: Relationship between computed tomographic image analysis and histomorphometry for microarchitectural characterization of human calcaneus. Calcif Tissue Int 75: 23-31, 2004.
71. Torres A, Lorenzo V and Gonzalez-Posada JM: Comparison of histomorphometry and computerized tomography of the spine in quantitating trabecular bone in renal osteodystrophy. Nephron 44: 282-287, 1986.
72. Park SB, Lee YJ and Chung CK: Bone mineral density changes after ovariectomy in rats as an osteopenic model: Stepwise description of double dorso-lateral approach. J Korean Neurosurg Soc 48: 309-312, 2010.
73. Laib A, Kumer JL, Majumdar S and Lane NE: The temporal changes of trabecular architecture in ovariectomized rats assessed by MicroCT. Osteoporos Int 12: 936-941, 2001.
74. Bouxsein ML, Boyd SK, Christiansen BA, Guldberg RE, Jepsen KJ and Müller R: Guidelines for assessment of bone microstructure in rodents using micro-computed tomography. J Bone Miner Res 25: 1468-1486, 2010.
75. Wu Y, Adeeb S and Doschak MR: Using Micro-CT derived bone microarchitecture to analyze bone stiffness-a case study on osteoporosis rat bone. Front Endocrinol (Lausanne) 6: 80, 2015.
76. Lee KY, Kim JH, Kim EY, Yeom M, Jung HS and Sohn Y: Water extract of Cnidii Rhizoma suppresses RANKL-induced osteoclastogenesis in RAW 264.7 cell by inhibiting NFATc1/c-Fos signaling and prevents ovariectomized bone loss in SD-rat. BMC Complement Altern Med 19: 207, 2019.
77. Lee K, Chung YH, Ahn H, Kim H, Rho J and Jeong D: Selective regulation of MAPK signaling mediates RANKL-dependent osteoclast differentiation. Int J Biol Sci 12: 235-245, 2016.
78. Yang JH, Li B, Wu Q, Lv JG and Nie HY: Echinocystic acid inhibits RANKL-induced osteoclastogenesis by regulating NF-κB and ERK signaling pathways. Biochem Biophys Res Commun 477: 673-677, 2016.
79. Xie BP, Shi LY, Li JP, Zeng Y, Liu W, Tang SY, Jia LJ, Zhang J and Gan GX: Oleanolic acid inhibits RANKL-induced osteoclastogenesis via ER alpha/miR-503/RANK signaling pathway in RAW264.7 cells. Biomed Pharmacother 117: 109045, 2019.